



Published in final edited form as:

Transl Neurosci. 2013 September 1; 4(3): . doi:10.2478/s13380-013-0132-3.

CHARACTERIZING CALCIUM INFLUX VIA VOLTAGE- AND LIGAND-GATED CALCIUM CHANNELS IN EMBRYONIC ALLIGATOR NEURONS IN CULTURE

Weina Ju^{1,§,#}, Jiang Wu^{§,#}, Michael B. Pritz^{1,2,4,*a}, and Rajesh Khanna^{1,3,4,5,*}

¹Paul and Carole Stark Neurosciences Research Institute, Indiana University School of Medicine, Indianapolis, IN 46202, USA

²Department of Neurological Surgery, Indiana University School of Medicine, Indianapolis, IN 46202, USA

³Department of Pharmacology and Toxicology, Indiana University School of Medicine, Indianapolis, IN 46202, USA

⁴Department of Anatomy and Cell Biology, Indiana University School of Medicine, Indianapolis, IN 46202, USA

⁵Indiana Spinal Cord and Brain Injury Research Group, Indiana University School of Medicine, Indianapolis, IN 46202, USA

[§]Department of Neurology, The First Hospital of Jilin University, Jilin University, Xinmin Street 71

[#]Changchun, 130021, Jilin Province, China

Abstract

Vertebrate brains share many features in common. Early in development, both the hindbrain and diencephalon are built similarly. Only later in time do differences in morphology occur. Factors that could potentially influence such changes include certain physiological properties of neurons. As an initial step to investigate this problem, embryonic *Alligator* brain neurons were cultured and calcium responses were characterized. The present report is the first to document culture of *Alligator* brain neurons in artificial cerebrospinal fluid (ACSF) as well as in standard mammalian tissue culture medium supplemented with growth factors. *Alligator* brain neuron cultures were viable for at least 1 week with unipolar neurites emerging by 24 hours. Employing Fura-2 AM, robust depolarization-induced calcium influx, was observed in these neurons. Using selective blockers of the voltage-gated calcium channels, the contributions of N-, P/Q-, R-, T-, and L-type channels in these neurons were assessed and their presence documented. Lastly, *Alligator* brain neurons were challenged with an excitotoxic stimulus (glutamate + glycine) where delayed calcium deregulation could be prevented by a classical NMDA receptor antagonist.

© Versita Sp. z o.o.

*michael.pritz@denlabs.com; khanna5@iu.edu.

^aPresent address:

Krasnow Institute for Advanced Study, Department of Molecular Neuroscience, George Mason University, Fairfax, VA 22030

Author Contributions:

All authors had full access to all the data in the study and take responsibility for the integrity of the data and the accuracy of the data analysis. Study concept and design: MBP, RK. Acquisition of data: WJ, MBP, RK. Analysis and interpretation of data: WJ, RK. Writing draft of manuscript: MBP, RK. Critical revision: MBP, RK. Statistical analysis: JW, RK.

Keywords

Alligator; Calcium mobilization; Immunoblot; Neuronal culture; NMDA receptor; Voltage-gated calcium channels

All vertebrate brains share many features in common and yet display a number of distinct differences. In vertebrate embryos, before internal subdivisions are present within major brain areas, early hindbrain and forebrain segments are built similarly [1,2]. Only later in development do changes occur which establish the pattern for the various different morphologies seen in the brains of adult species. Documentation to explain the mechanisms as well as the morphological differences of these various brain regions remains incomplete.

Although not unequivocally established experimentally, certain physiological properties of both embryonic and adult neurons are assumed to be similar. In vertebrate brains, free calcium ions are biologically active, are crucial to neuronal function [3], and are presumably present and function intracellularly in a similar fashion in both adult and embryonic neurons. Accordingly, calcium channels and responses to an excitotoxic stimulus should be common features of all neurons.

Reptilian brains in general, and crocodilian brains in particular, are of interest from a physiological perspective that has direct translational importance. Poikilotherms, “cold blooded vertebrates”, are well known to tolerate prolonged periods of hypoxia with little to no obvious brain damage or behavioral changes [4]. For example, *in vitro* preparations of eyes and a whole brain in turtles can survive for hours with physiological responses similar to *in vivo* conditions as long as satisfactory nutrients and oxygen are supplied [5]. Moreover, certain poikilotherms can be cooled to such low core-body temperatures that brainstem functions are lost, only to have these functions return after re-warming. These observations formed the basis for cold narcosis that has been used in the past for anesthesia on certain crocodilians [6].

Although the mechanisms, cellular processes, and expression of genes that explain both the vulnerability and lack of vulnerability of neurons to hypothermia and, presumably hypoxia, are incompletely known, intracellular calcium accumulation is one factor critical to neuronal death and survival [7,8]. Thus, examination of calcium channels and the response to an excitotoxic stimulus was considered to be an initial first step.

Materials and Methods

Specimens

Alligator mississippiensis eggs were obtained from the Rockefeller Wildlife Refuge in Grand Chenier, Louisiana, and were housed in an incubator at 30°C. Embryos were removed from eggs and staged [9]. Five brains were used at the following stages: stage 16 (N=1) and stage 19 (N=4). After staging, animals were euthanized by occipito-cervical transection. Brains were placed in a solution of 5% glycerol and artificial cerebrospinal fluid and stored at -80°C until tissue was processed. Brains from gestational day 14 chicken eggs (Pearl white leghorn, Charles River) and embryonic day 19 Sprague Dawley rats were isolated and flash frozen until analysis.

Culture of Alligator neurons

Stage 16 and 19 *Alligator* brains were collected on ice in filtered artificial cerebrospinal fluid (ACSF) which contained 100 mM NaCl, 6 mM KCl, 1.6 mM MgCl₂, 40 mM NaHCO₃, 20 mM Glucose, and 2.6 mM CaCl₂. The brains were then transferred to a

dissociation enzyme cocktail containing 1 µg/ml dispase (a metallo, neutral protease; Worthington Biochemical Corporation, Lakewood, NJ) and 1.67 µg/ml collagenase (Worthington Biochemical Corporation) in ACSF and incubated for 10 min at 37°C. Then, the brain/dissociation enzyme cocktail was gently mechanically sheared by pipetting it through a 200 µl Eppendorf pipette at least 3 times and returned to 37°C for another 15 min. The pellet was resuspended in bicarbonate free, serum free, sterile Dulbecco's modified Eagle's medium (bfDMEM; pH=7.3), centrifuged at 500 ×g for 2 min to remove the enzyme-containing supernatant and mechanically dissociated with fire-polished pipettes with a decreasing inner tip diameter. The resulting suspension of single cells was plated on poly-D-lysine-coated coverslips and maintained in Dulbecco's modified Eagle's medium (DMEM) (Gibco, Invitrogen, Grand Island, NY, USA). The *Alligator* brains were grown in a humidified incubator in DMEM supplemented with 10% fetal bovine serum (FBS) (Hyclone, Logan, UT, USA) and NGF (30 µg/ml; Harlan Bioproducts, Indianapolis, IN, USA) at 37°C in a 5% CO₂ atmosphere.

Fura-2-AM calcium imaging

Ratiometric Ca²⁺ imaging was performed as described previously [10–13] on *Alligator* neurons that were cultured for 12–24 h following isolation. Briefly, neurons were loaded with 3 µM Fura-2AM (in Tyrode's buffer: 119mM NaCl, 2.5mM KCl, 2mM CaCl₂, 2mM MgCl₂, 25mM HEPES pH 7.4, 30mM Glucose) for 30 min at 37° Celsius in the dark. Neurons were then washed 1× with Tyrode's buffer before transferring cells to the imaging stage. Cell fluorescence was measured by digital video microfluorometry with an intensified CCD camera coupled to a microscope and Nikon Elements Software (Nikon Instruments Inc., Melville, NY, USA). Cells were illuminated with a Lambda DG-4 175 W Xenon lamp, and the excitation wavelengths of the Fura-2 (340/380 nm) were selected by a filter changer. Fura-2 fluorescence (F340/ F380) was measured every 2.1 seconds to minimize photo-bleaching. After a baseline of at least 1 min was obtained, neurons were stimulated by addition of excitatory Tyrode's buffer (32mM NaCl, (45mM) or 90mM KCl, 2mM CaCl₂, 2mM MgCl₂, 25mM HEPES pH 7.4, 30mM Glucose), excitatory Tyrode's buffer with 300 nM Agatoxin, excitatory Tyrode's buffer with 150 nM SNX-482, excitatory Tyrode's buffer with 1 µM Conotoxin, excitatory Tyrode's buffer with 100µM Mibefradil, excitatory Tyrode's buffer with 100µM CdCl₂, excitatory Tyrode's buffer with 5µM Isradipine, or normal Tyrode's buffer with 200 µM Glutamate and 20 µM Glycine with or without MK-801. Depolarization was evoked with a 10 s pulse of 90 mM potassium chloride delivered via a Valvelink 8.1 controlled gravity-driven perfusion system (Automate Scientific, Berkeley, CA, USA).

Isolation of brain lysates and immunoblotting

Alligator (stage 19), chicken or rat brain lysates were generated by homogenization and gentle sonication in a detergent free modified RIPA buffer (50 mM Tris-HCl, pH=8, 1% nonidet P-40 (NP-40/Igepal), 150 mM NaCl, 0.5% Na deoxycholate, and 1 mM EDTA, and supplemented with freshly added protease inhibitors: 1 µg/ml leupeptin, 1 µg/ml aprotinin, 1 µg/ml pepstatin, 1 mM PMSF (Sigma-Aldrich, St. Louis, MO, USA) together with a protease inhibitor cocktail (Roche Applied Science, Laval, Quebec)). The protein concentration of all samples was determined by BCA protein assay (Thermo Scientific, West Palm Beach, FL, USA). Immunoblotting was performed exactly as described [14–17].

Results

Derivation and culture of *Alligator* brain neurons

Following aseptic dissection, *Alligator* brain neurons were plated in medium optimized for mammalian cells (Figure 1A) or in ACSF supplemented with fetal bovine serum (Figure

1B). Greater than 90% of the cells were viable as assessed by their exclusion of the vital dye trypan blue. In the glass bottom culture dishes, the cells settled rapidly from the suspension, attached to the poly-D-lysine substrate, and extended short processes within the first 12 h of culture (Figure 1). This was followed by the emergence of one to two neurites, which extended in length and began to branch out over the next 24–36 h. In this early phase of the cultures, fibroblast-like cells were largely absent (but see examples in Figure 2A). The neurons grown in ACSF medium tended to aggregate over time, which lead to rapid deterioration of cell health and eventual death. In contrast, neurons grown in mammalian cell culture medium appeared healthy and survived for up to 1 week in culture. Although glial cells were also observed in our cultures, based on morphology alone, neurons could be reliably discerned.

Depolarization-evoked Ca^{2+} influx in *Alligator* brain neurons

In order to determine whether the *Alligator* brain neurons were functional, calcium imaging was performed using the ratio-metric dye Fura-2-AM, which has been extensively used to measure intracellular calcium elevations in neurons and other excitable cells. These early experiments used *Alligator* brain neurons grown in ACSF medium. Stimulation with low (45 mM potassium chloride (KCl)) or high (90 mM potassium chloride (KCl)) led a rapid increase in the Fura-2-AM ratio (Figure 2A, 45 mM K^+ and 90 mM K^+ panels) which indicated an increase in intracellular calcium concentration ($[\text{Ca}^{2+}]_i$) in these neurons. Figure 2B and C illustrate the range of responses to 45 mM K^+ and 90 mM K^+ , respectively. Verification that the observed fluorescence ratio changes were due to calcium influx via voltage-gated calcium channels was documented by the ~85% reduction in peak calcium influx in the presence of the non-specific calcium channel blocker cadmium chloride (100 μM CdCl_2 ; Figure 2D), as assessed via analyzing area under the curve (AUC). For the AUC measurements, the area above baseline $[\text{Ca}^{2+}]_i$ was used rather than the area above the x-axis, as the aim was to assess net response to the agonist rather than total Ca^{2+} activity. Stimulation with 90 mM K^+ induced an ~3-fold greater calcium influx than 45 mM K^+ (Figure 2E); calcium influx triggered by both paradigms was inhibited (>85% by inclusion of 100 μM CdCl_2 (data not shown for the 45 mM KCl condition).

The same set of experiments in *Alligator* brain neurons described above was repeated in cells grown in mammalian cell culture medium. As before, both low and high potassium stimulation paradigms elicited robust and reproducible increases in calcium influx (Figure 3A–C). Inclusion of 100 μM CdCl_2 in the bath at time of stimulation with 90 mM K^+ led to an ~84% suppression of calcium influx (Figure 3C,D). Stimulation with 90 mM K^+ recapitulated the ~3-fold greater calcium influx than 45 mM K^+ observed in neurons grown in ACSF medium (Figure 3D).

Blockers of voltage-gated calcium channels reduce depolarization-evoked Ca^{2+} influx

Because the *Alligator* neurons grown in mammalian cell culture medium appeared healthier than those in ACSF culture, these cells were utilized to dissect the route of calcium entry into these neurons. As illustrated in Figure 4, neurons were challenged sequentially, approximately 1 min apart, with Tyrode's buffer containing 90 mM K^+ , 90 mM K^+ plus specific blockers of voltage-gated calcium channels, and finally 90 mM K^+ plus 100 μM CdCl_2 . Figure 4 depicts the averaged time courses of the responses of these neurons (left panels) and the average AUCs (bar graphs in right panels). Incubation with 1 μM omega-conotoxin (-CTX; N-type selective calcium channel blocker; Figure 4A) inhibited calcium influx by ~30%; 300 nM omega-agatoxin (-AgTx, P/Q-type selective calcium channel blocker; Figure 4B) inhibited calcium influx by ~27%; 150 nM SNX-482 (R-type selective calcium channel blocker; Figure 4C) inhibited calcium influx by ~52%; 100 μM Mibefradil (Mibefradil, T-type selective calcium channel blocker; Figure 4D) inhibited calcium influx

by ~65%; and 5 μM Isradipine (Isradipine, L-type selective calcium channel blocker; Figure 4E) inhibited calcium influx by ~34%. While a combinatorial block was not tested, these results suggest that *Alligator* brain neurons possess all major voltage-gated calcium channels.

NMDAR blockade reduces glutamate-induced Ca^{2+} influx

Next, the expression of functional ligand-gated ion channels such as the NMDAR was examined for *Alligator* brain neurons. Challenging neurons with NMDAR agonists glutamate (200 μM) and glycine (20 μM) led to a slow unchecked rise in calcium (Figure 5A,C), reminiscent of the delayed calcium deregulation that occurs in mammalian neurons following such stimulation. Incubation with the NMDAR blocker MK-801 (50 μM) suppressed the peak calcium influx by ~65% (Figure 5B,C). These results suggest that *Alligator* brain neurons express functional NMDARs that behave in a very similar fashion to their mammalian counterparts.

Comparing expression of select proteins between *Alligator*, chicken, and rat brains

We finally tested the expression of a small subset of proteins that are predicted to share high homology between species, namely, (i) the NMDAR, (ii) an axonal growth and guidance collapsin response mediator protein 2 (CRMP2), which we have previously shown to regulate NMDARs, (iii) the general neuronal cytoskeletal protein α -tubulin, and (iv) the presynaptic protein syntaxin. Levels of all four proteins tested were relatively similar between *Alligator*, chicken, and rat brains. Notably, a faster migrating band (at ~150 kDa) was observed in *Alligator* brains for the NMDAR – this could represent a truncated form of the receptor or an alternatively spliced product that does not exist in avian or mammalian species.

Discussion

As an initial step in examining certain physiological properties of cultured embryonic neurons in a crocodylian, the present series of experiments have documented three important and significant results. First, embryonic *Alligator* neurons were not only able to be successfully cultured but also to be maintained over several days. Support for this is two-fold: images of neurons in culture (Figure 1) that demonstrate neuronal processes and appearance similar to that of cultured mammalian and chick neurons and robust depolarization-induced calcium influx, using Fura-2 AM (Figure 2). Second, calcium channel subtypes commonly found in other species [18,19] were demonstrated in these cultured *Alligator* neurons. Using selective blockers, the N-, P/Q-, R-, T, and L-type voltage gated calcium channels were demonstrated. Third, challenge of *Alligator* brain neurons with an excitotoxic stimulus (glutamate + glycine) showed delayed calcium deregulation that could be prevented by a classical NMDA receptor antagonist. Consistent with this data, the levels of the NR2B subunit of the NMDA receptor are not different between reptilian, avian or mammalian brains.

Taken together, at the stages of development examined, cultured *Alligator* neurons display biologically important properties common to similarly cultured brain neurons in other amniotes. While these results may not be surprising, these data provide a foundation for more specific questions that could not have been addressed without these basic observations.

From a physiologic standpoint, do cultured embryonic *Alligator* neurons resist a challenge to hypoxia? Do these properties change as development proceeds? Are some brain regions more vulnerable than others? Additionally, it would be of interest to characterize alternative routes of calcium influx, intracellular pathways, as well as efflux pathways using

pharmacological inhibitors. Additionally, whole-cell patch clamp electrophysiology could be applied to further test the biophysical properties of calcium influx via the voltage-gated calcium channels.

Answers to these questions should provide biologically significant information from a naturally occurring animal model system that has successfully tolerated hypothermia and degrees of hypoxia. Additional data on the potential lack of vulnerability of cultured neurons to hypoxia would have potential direct translational application and perhaps, begin to unravel as to why some neurons are sensitive to hypoxia while others are not.

Acknowledgments

Dr. Joel M. Brittain and Sarah Marie Wilson provided technical assistance; Dr. Fletcher A. White lent us the use of his calcium imaging microscope; and Dr. R. M. Elsey of the Rockefeller Wildlife Refuge generously provided *Alligator* eggs. Partial support for this publication was provided by: a Project Development Team grant within the ICTSI NIH/NCRR Grant Number RR025761 (to R.K.); grants from the Ralph W. and Grace M. Showalter foundation (to R.K.), and the Elwert Award in Medicine (to R.K.). W.J. is partially supported by a State Scholarship Fund issued by the Graduate Training Department of Jilin University.

References

1. Pritz MB. Rhombomere development in a reptilian embryo. *J. Comp. Neurol.* 1999; 411:317–326. [PubMed: 10404256]
2. Pritz MB. Early diencephalon development in alligator. *Brain Behav. Evol.* 2008; 71:15–31. [PubMed: 17878715]
3. Grienberger C, Konnerth A. Imaging calcium in neurons. *Neuron.* 2012; 73:862–885. [PubMed: 22405199]
4. Bickler PE. Clinical perspectives: neuroprotection lessons from hypoxia-tolerant organisms. *J. Exp. Biol.* 2004; 207:3243–3249. [PubMed: 15299045]
5. Mancilla JG, Fowler M, Ulinski PS. Responses of regular spiking and fast spiking cells in turtle visual cortex to light flashes. *Vis. Neurosci.* 1998; 15:979–993. [PubMed: 9764539]
6. Pritz MB. Interconnections between the dorsal column nucleus and the cerebellum in a reptile. *Neurosci. Lett.* 2011; 495:183–186. [PubMed: 21440041]
7. Buck LT, Bickler PE. Adenosine and anoxia reduce n-methyl-d-aspartate receptor open probability in turtle cerebrocortex. *J. Exp. Biol.* 1998; 201:289–297. [PubMed: 9405320]
8. Deshpande JK, Siesjö BK, Wieloch T. Calcium accumulation and neuronal damage in the rat hippocampus following cerebral ischemia. *J. Cereb. Blood Flow Metab.* 1987; 7:89–95. [PubMed: 3805166]
9. Ferguson MW. Reproductive biology and embryology of the crocodylians. *Biology of the Reptilia.* 1985; 14:329–491.
10. Brittain JM, Duarte DB, Wilson SM, Zhu W, Ballard C, Johnson PL, et al. Suppression of inflammatory and neuropathic pain by uncoupling CRMP-2 from the presynaptic Ca²⁺ channel complex. *Nat. Med.* 2011; 17:822–829. [PubMed: 21642979]
11. Ju W, Li Q, Allette YM, Ripsch MS, White FA, Khanna R. Suppression of pain-related behavior in two distinct rodent models of peripheral neuropathy by a homopolyarginine-conjugated CRMP2 peptide. *J. Neurochem.* 2012; 124:869–879. [PubMed: 23106100]
12. Ju W, Li Q, Wilson SM, Brittain JM, Meroueh L, Khanna R. SUMOylation alters CRMP2 regulation of calcium influx in sensory neurons. *Channels (Austin).* 2013; 7:153–159. [PubMed: 23510938]
13. Wilson SM, Schmutzler BS, Brittain JM, Dustrude ET, Ripsch MS, Pellman JJ, et al. Inhibition of transmitter release and attenuation of aids therapy-induced and tibial nerve injury-related painful peripheral neuropathy by novel synthetic Ca²⁺ channel peptides. *J. Biol. Chem.* 2012; 287:35065–35077. [PubMed: 22891239]

14. Brittain JM, Chen L, Wilson SM, Brustovetsky T, Gao X, Ashpole NM, et al. Neuroprotection against traumatic brain injury by a peptide derived from the collapsin response mediator protein 2 (CRMP2). *J. Biol. Chem.* 2011; 286:37778–37792. [PubMed: 21832084]
15. Brittain JM, Piekarz AD, Wang Y, Kondo T, Cummins TR, Khanna R. An atypical role for collapsin response mediator protein 2 (CRMP-2) in neurotransmitter release via interaction with presynaptic voltage-gated calcium channels. *J. Biol. Chem.* 2009; 284:31375–31390. [PubMed: 19755421]
16. Brittain JM, Wang Y, Eruvwetere O, Khanna R. Cdk5-mediated phosphorylation of crmp-2 enhances its interaction with cav2.2. *FEBS Lett.* 2012; 586:3813–3818. [PubMed: 23022559]
17. Chi XX, Schmutzler BS, Brittain JM, Hingtgen CM, Nicol GD, Khanna R. Regulation of N-type voltage-gated calcium (Cav2.2) channels and transmitter release by collapsin response mediator protein-2 (CRMP-2) in sensory neurons. *J. Cell Sci.* 2009; 23:4351–4362. [PubMed: 19903690]
18. Catterall WA. Voltage-gated calcium channels. *Cold Spring Harb. Perspect. Biol.* 2011; 3:a003947. [PubMed: 21746798]
19. Dolphin AC. Calcium channel diversity: multiple roles of calcium channel subunits. *Curr. Opin. Neurobiol.* 2009; 19:237–244. [PubMed: 19559597]

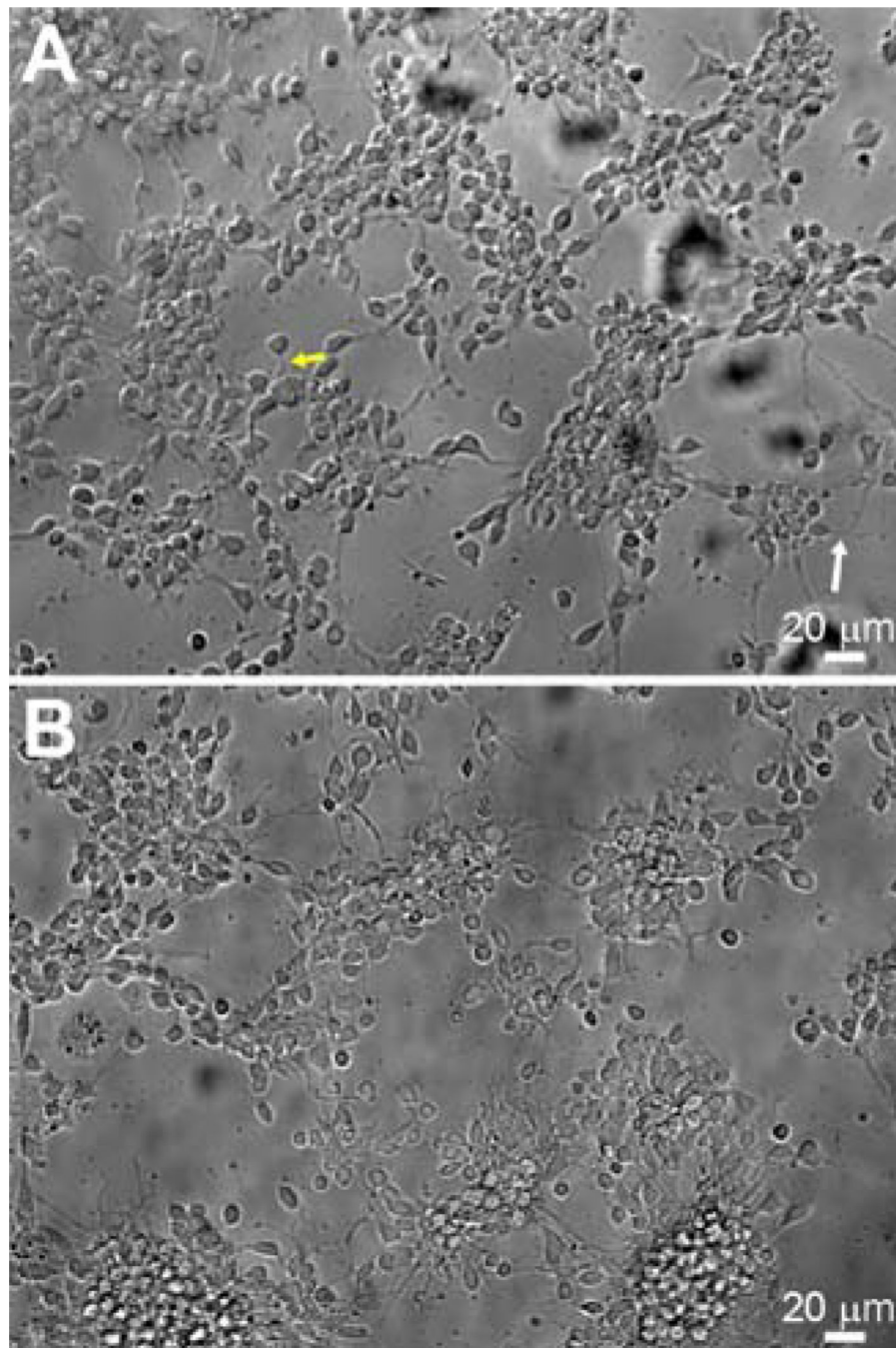


Figure 1. Differential interference contrast (DIC) images of *Alligator* brain neurons during the first 24 h of culture grown in mammalian cell culture media (A) or ACSF supplemented with serum (B). Yellow arrow indicates an emerging neurite while the white arrow likely represents an axon, typified by a sharp right angle turn from its short neurite. Scale bars are as indicated.

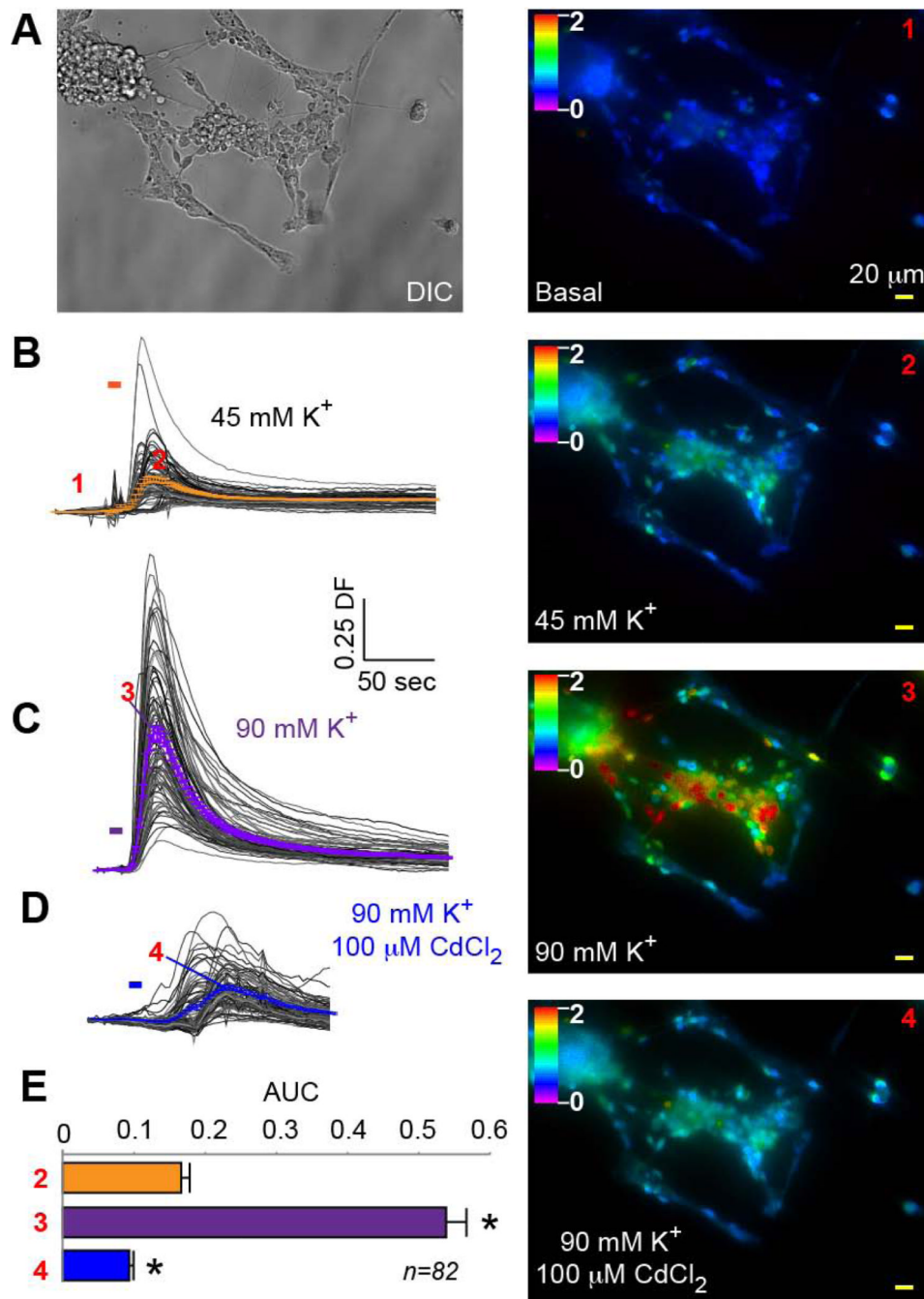


Figure 2. Analysis of area under the curve (AUC) in Fura-2-AM-loaded *Alligator* brain neurons. (A) Differential interference contrast (DIC) and pseudocolored fluorescent images of a field of dissociated *Alligator* brain neurons and fibroblasts at rest (Basal, 1), following stimulation with KCl (45 mM K⁺, 2 or 90 mM K⁺, 3) or in the presence of the general calcium channel blocker cadmium chloride (100 μM CdCl₂, 4). The color scale indicates that the resting cytoplasmic calcium concentration is relatively low (magenta and blue). The color scale, same for all colored panels, indicates that the cytoplasmic calcium concentration is relatively high in many cells (green, yellow, and red) following stimulation. Scale bar: 20 μm. Glial cells did not respond to 90 mM KCl with elevated cytoplasmic calcium. Time course of

calcium responses following stimulation with KCl (45 mM K⁺ (B)) or 90 mM K⁺, (C)) or in the presence of the general calcium channel blocker cadmium chloride (D). The colored traces represent the averaged traces with standard errors. Values represent n = 82 cells obtained from two separate experiments for each treatment. (E) Illustration of the [Ca²⁺]_i signaling AUC assessed for 75 s in response to depolarizing stimuli with and without blocker. Note that the area above baseline [Ca²⁺]_i is used rather than the area above the x-axis, as the aim was to assess net response to the agonist rather than total Ca²⁺ activity. Asterisks indicate statistical significance compared with the 45 mM KCl condition (p < 0.05, one-way ANOVA with Dunnett's post-hoc test). Numbers in parentheses represent the numbers of cells tested in each condition.

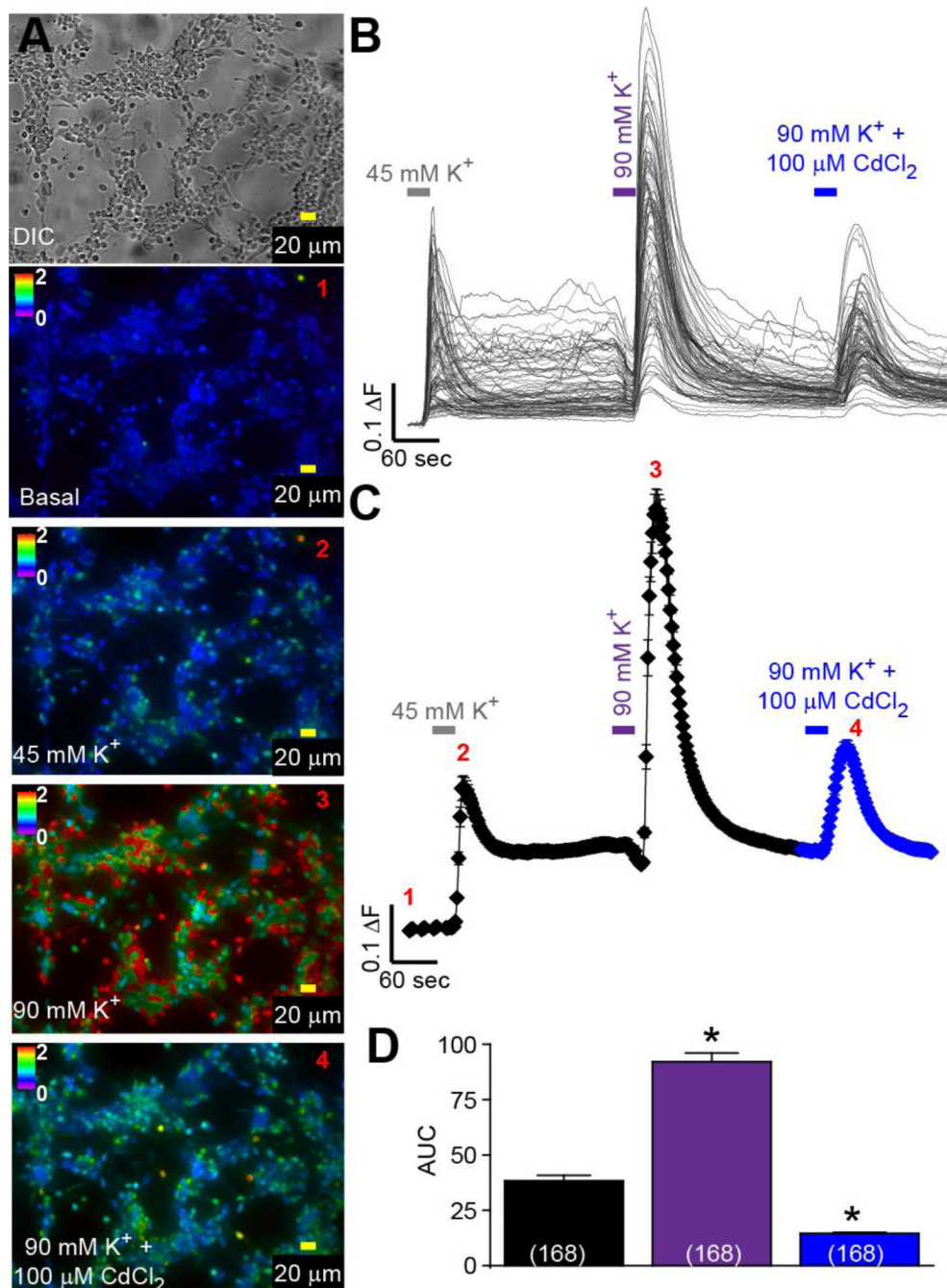


Figure 3. Calcium responses of *Alligator* brain neurons cultured in mammalian cell culture medium. (A) Differential interference contrast (DIC) and pseudocolored fluorescent images of a field of dissociated *Alligator* brain neurons and fibroblasts at rest (Basal, 1), following stimulation with KCl (45 mM K⁺, 2 or 90 mM K⁺, 3) or in the presence of the general calcium channel blocker cadmium chloride (100 μM CdCl₂, 4). Additional details exactly as those in the legend to Figure 2. Individual time course (B) and averages (C) of calcium responses of all cells responding to sequential application of 45 mM K⁺, 90 mM K⁺, and then 90 mM K⁺ plus 100 μM CdCl₂. (D) Bar graphs showing the area under the curve (AUC) fluorescence responses ± s.e.m. (adjusted for background) of *Alligator* brain neurons.

Asterisks indicate statistical significance compared with the 45 mM KCl condition ($p < 0.05$, one-way ANOVA with Dunnett's post-hoc test). Numbers in parentheses represent the numbers of cells tested in each condition.

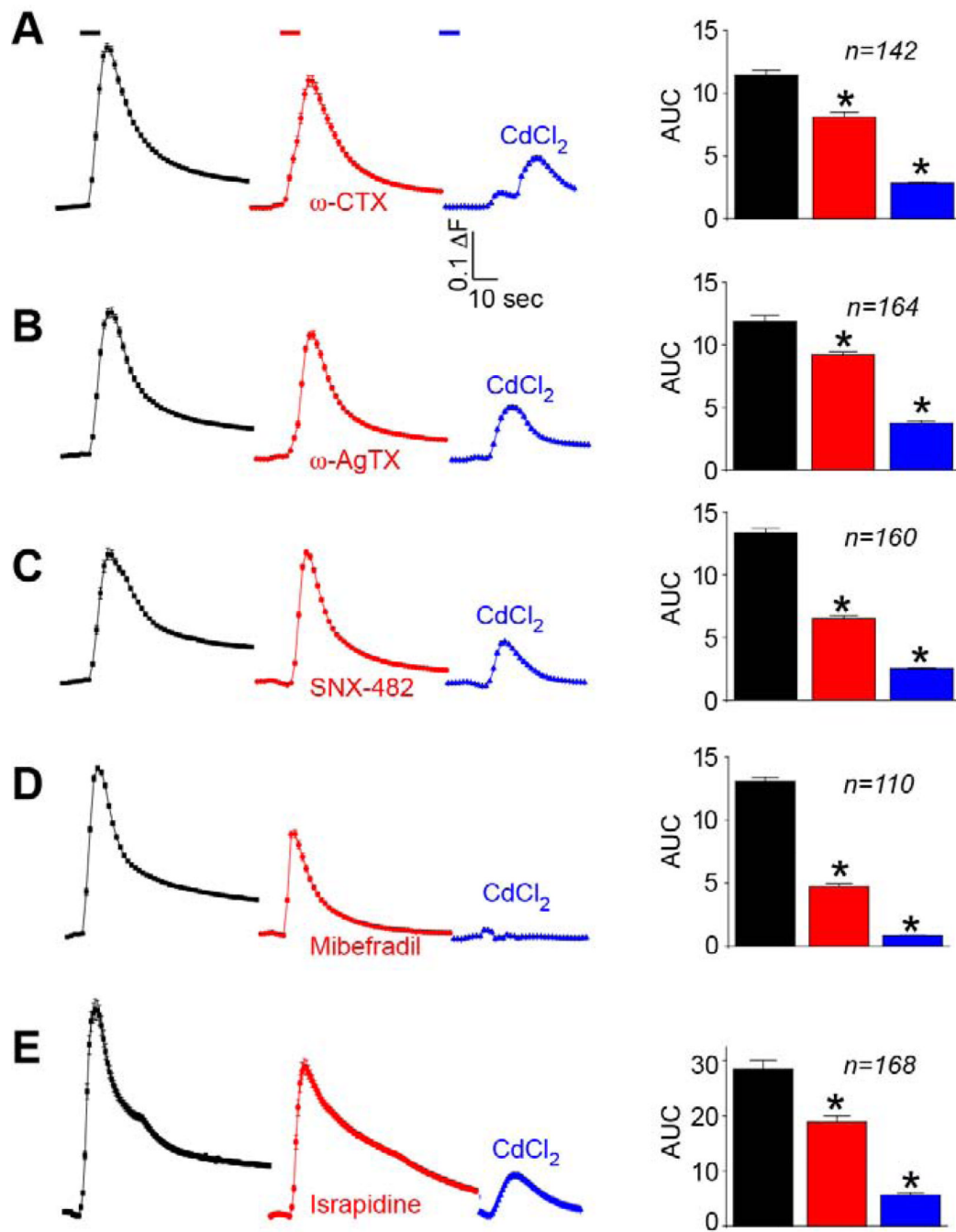


Figure 4. Blockers of voltage-gated calcium channels reduce depolarization-evoked Ca²⁺ influx in *Alligator* brain neurons. Averaged calcium time dependent responses of all cells responding to sequential application of 90 mM K⁺ (black), 90 mM K⁺ + selective calcium channel blockers (red), and finally 90 mM K⁺ plus 100 μM CdCl₂. Bar graphs showing the area under the curve (AUC) fluorescence responses ± s.e.m. (adjusted for background) of *Alligator* brain neurons are shown on the right of each panel. Asterisks indicate statistical significance compared with the 90 mM KCl condition (p < 0.05, one-way ANOVA with Dunnett's post-hoc test). Numbers in italics represent the numbers of cells tested in each

condition. Calcium responses returned to within 5–10% of baseline prior to initiation of the subsequent depolarizing challenges.

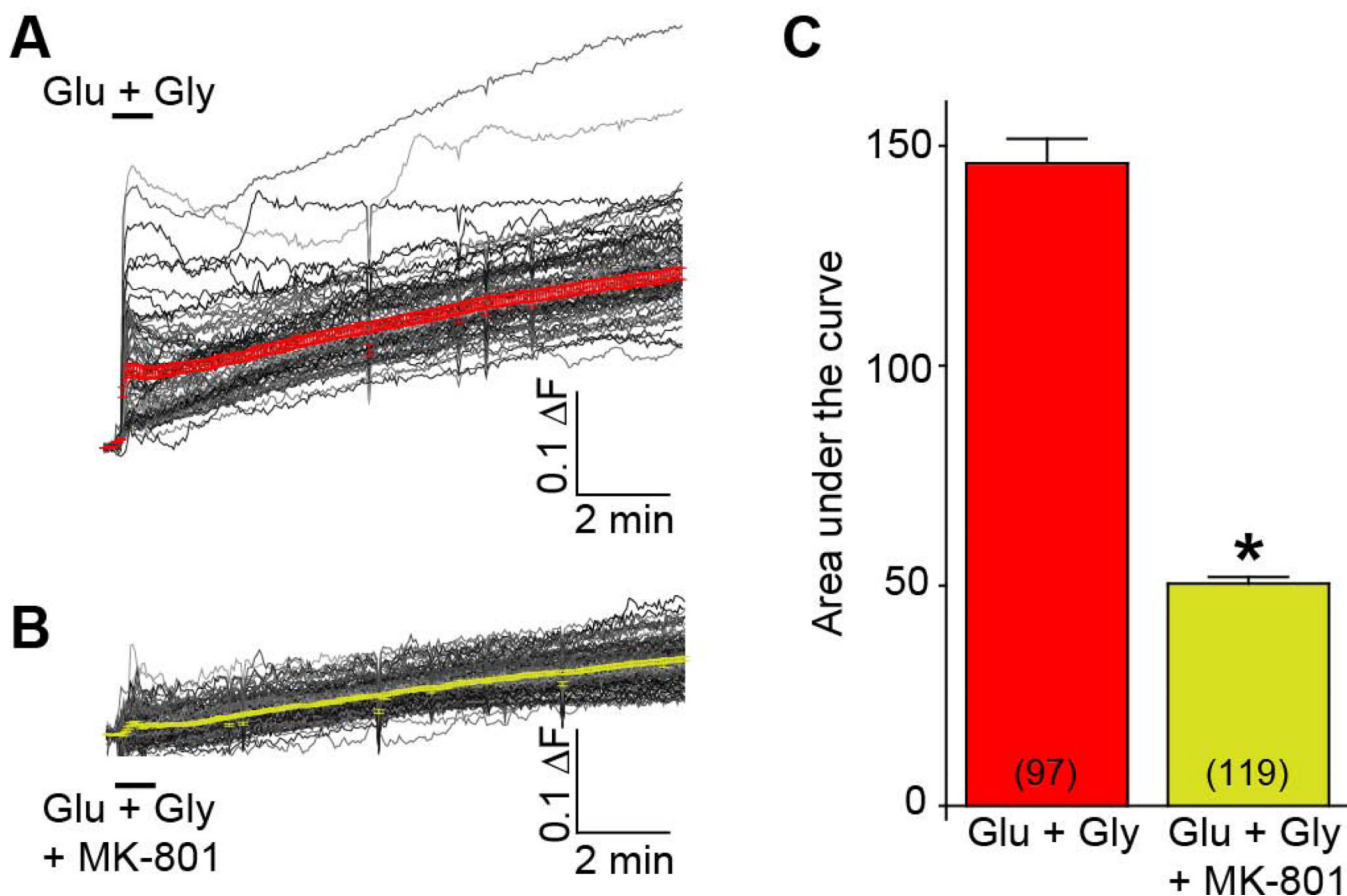


Figure 5. Glutamate-induced delayed calcium-dysregulation is conserved in *Alligator* brain neurons. $[Ca^{2+}]_c$ was monitored in *Alligator* brain neurons after exposure to 200 μ M glutamate + 20 μ M glycine using the Ca^{2+} -sensitive Fura-2AM. The calcium response of neurons (black traces) and their averages (colored traces) challenged with excitotoxic stimulus (Glu+ Gly) in the absence (vehicle – 0.05% DMSO, A) or in the presence of the NMDA receptor blocker (50 μ M MK-801, B) are shown. C) Bar graph illustrating the $[Ca^{2+}]_i$ signaling area under the curve (in arbitrary units) assessed for 10 min in response to stimuli with and without blocker. Asterisk indicates statistical significance compared with control ($p < 0.05$, Student's t-test). Numbers in parentheses represent the numbers of cells tested in each condition.

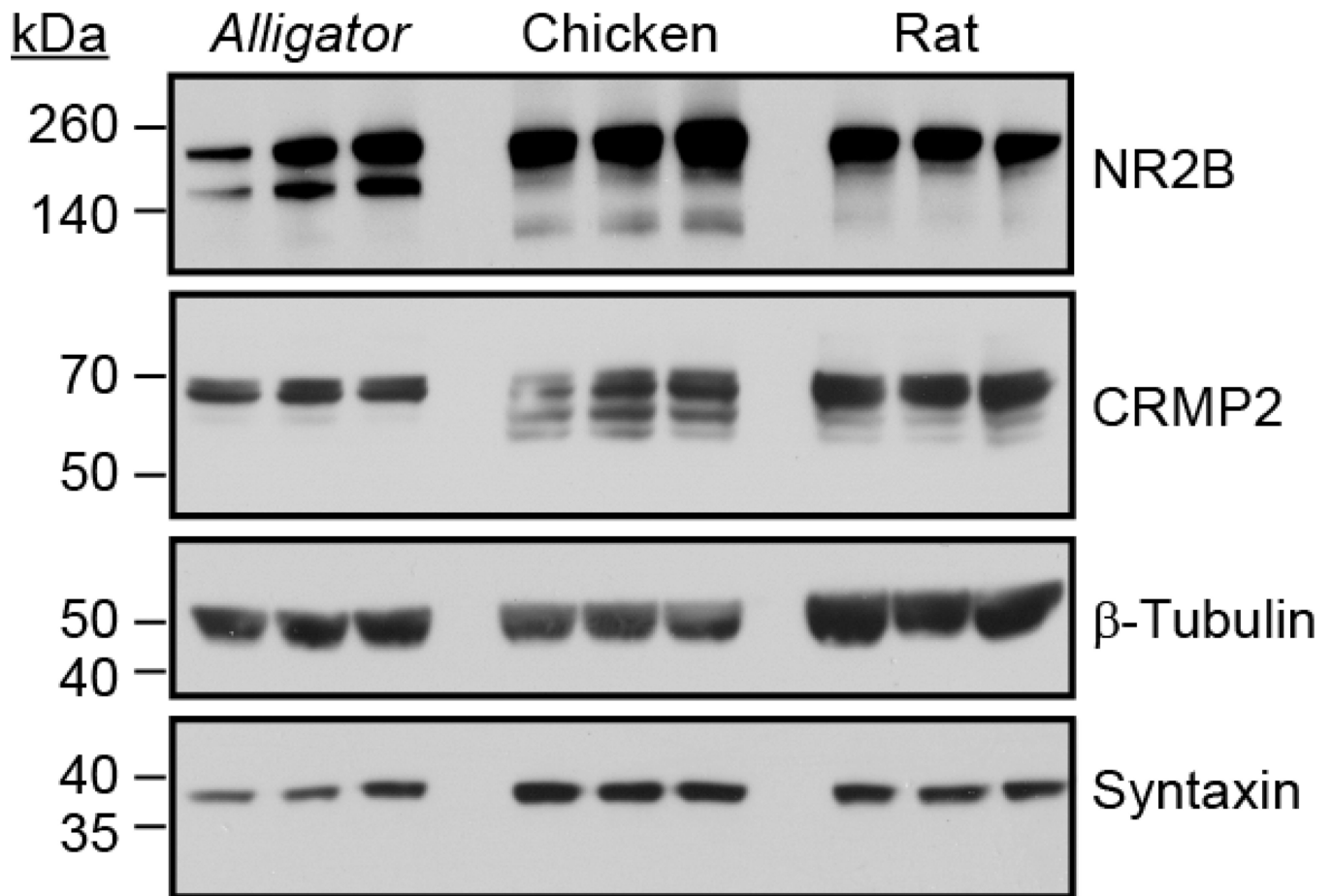


Figure 6.

Expression of a subset of membrane and cytosolic protein in embryonic *Alligator* brains, gestational day 14 chick brains, and embryonic day 19 rats. Immunoblot analyses of equal amounts of protein were immunoblotted with the indicated antibodies. Three independent samples for each species are shown. Levels of all four proteins tested were relatively similar between *Alligator*, chicken, and rat brains. Molecular weights in kilodaltons (kDa) are indicated.

Table 1

Antibodies used in this study.

Antibody	Source	WB
CRMP2 (p) ^a	Sigma	1:1000
NR2B (m)	BD Biosciences	1:1000
Syntaxin (m)	Sigma clone HPC-1	1:1000
-tubulin (m)	Promega	1:2000

^aAbbreviations used: WB, Western blot; m, monoclonal; p, polyclonal; CRMP2, collapsin response mediator protein 2.